Energy Equip. Sys./ Vol. 6/No. 1/March 2018/ 101-116

ENERGY EQUIPSYS

Energy Equipment and Systems

http://energyequipsys.ut.ac.ir
www.energyequipsys.com

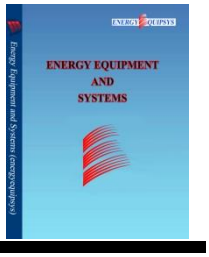

Optimizing the AGC system of a three-unequal-area hydrothermal system based on evolutionary algorithms

Authors

Ramin Sakipour[a]
Hamdi Abdi[a]*

[a] Electrical Engineering Department, Engineering Faculty, Razi University, Kermanshah, Iran

ABSTRACT

This paper focuses on expanding and evaluating an automatic generation control (AGC) system of a hydrothermal system by modelling the appropriate generation rate constraints to operate practically in an economic manner. The hydro area is considered with an electric governor and the thermal area is modelled with a reheat turbine. Furthermore, the integral controllers and electric governor parameters are optimized using integral squared error (ISE) criterion. Also, a novel Teaching-Learning-Based Optimization (TLBO) algorithm, Particle Swarm Optimization (PSO), and Gravitational Search Algorithm (GSA) with controller are proposed for optimizing AGC. Investigations have been conducted for the selection of a suitable value for governor speed regulation parameter R for the hydro and thermal areas, to explore the effect of tie-line power on the dynamic response. The advantages of the proposed approach are demonstrated by comparing the results of optimizing the AGC system of a three-unequal-area hydrothermal system with mentioned algorithms for the first one in comparison with other recently published techniques. The results confirm the flexibility and the suitability of the proposed AGC model for optimizing the different approaches. Moreover, it is more practical to use the proposed method to make a wide variety of changes in the system parameters using sensitivity analysis.

Article history:

Received : 30 October 2017
Accepted : 4 December 2017

Keywords: Automatic Generation Control (AGC), Multi-Area Hydrothermal System, Teaching-Learning-Based Optimization (TLBO), Particle Swarm Optimization (PSO), Gravitational Search Algorithm (GSA).

1. Introduction

Today's, ever-growing dependence on energy, especially in the form of electricity, confronts producers with different issues, which are related to some crucial matters in the field of power stability, load-frequency control (LFC), economical load-frequency distribution, and tracking trips. Generally, power systems are divided into various areas, each of which is commonly interconnected with its neighboring areas. The transmission lines that connect an area to its neighboring area are known as tie-lines. Power-sharing between two areas occurs through these tie-lines. LFC, as the name implies, regulates the power flow between different areas while holding the frequency constant. In other words, the LFC has two major objectives: The frequency constant ($\Delta f = 0$) must be held against any load change (each area must contribute to absorb any load change such that the frequency does not deviate), and

* Corresponding author: Hamdi Abdi
Electrical Engineering Department, Engineering Faculty, Razi University, Kermanshah, Iran
Email: hamdiabdi@razi.ac.ir

each area must maintain the tie-line power flow at its pre-specified value.

Due to these facts, automatic generation control (AGC) is one of the most effective methods proposed recently, which plays an important role in the large-scale multi-area interconnected power systems to maintain system frequency and tie-line powers at their nominal values. In an electric power system, AGC is a control system for adjusting the power output of multiple generators at an interconnected power system, in response to different changes in the load. Since a power grid requires that generation and load closely balance moment by moment, frequent adjustments to the output of generators are necessary. The balance can be judged by measuring the system frequency. On the other hand, if the generated active power becomes less than the power demand due to sudden disturbances, the frequency of generating units tends to decrease, and vice versa [1–3]. This makes the system frequency deviate from its nominal value, which is undesirable. To damp out the frequency deviation quickly and to keep the tie-line power at its scheduled value, the AGC system is employed [3].

However,it should be noted that the frequency cannot be fixed at a constant value by the governor, alone. So, a control system is essential to cancel the effects of the sudden load changes and to keep the frequency at the nominal value [3]. Although AGC is necessary to adapt and regulate active power and frequency simultaneously, this method should be optimized with control strategies and intelligent heuristic algorithms in order to make the results more reliable for companies and power plants.

Through the last few decades, the concepts of optimal control theory [4], integral [5], proportional integral [6], proportional-integral derivative [7], integral-double derivative [8], fractional-order PID [9], and proportional-integral-double derivative [10] have been widely applied and their performances have been compared for an AGC problem [3].

Accordingly, Daneshfar and Bervani [11] propose the multi-objective optimization problem (MOP) approach, which involves applying GA in order to tune PI controllers for multi-area power systems. Swasti and Panda [12] suggest an ANFIS-based approach to analyze the simulation of AGC in a multi-area power system. They introduced the application of ANN-based ANFIS approach to the AGC of a three-unequal-area hydrothermal system. The proposed ANFIS controller combines the advantages of fuzzy controller and the quick response and adaptable nature of ANN. They claim that their approach satisfies the LFC requirements with a reasonable dynamic response. In addition, Rabindra et al. in [3] propose optimizing the AGC of a two-area non-reheat thermal power system using the TLBO algorithm.

While studying the aforementioned proposed approaches, the results show the lack of efficient focusing on the studying of the AGC of multi-area power systems (three or more than three unequal areas). Also, in some case studies of multi-area systems, researchers insist on optimizing the complementary controller gains using ANN, hybrid GA-simulated annealing (GA-SA), or fuzzy-logic - based techniques [13,14]. Moreover, a large number of existing studies in the field of AGC consist of two interconnected equal-area thermal systems; little attention has been paid to the AGC of unequal multi-area systems. Further, in most of the recent studies, a two-area power system is discussed; their case studies usually involve thermal or hydro plants only [15–18].

In this paper, the case study includes a three-unequal-area power system with two thermal plants and a hydro plant, as originally introduced in [19]. However, for the purpose of achieving a better design, a MATLAB/Simulink model of the power system with its controllers is developed [12]. In addition, in this study, the Simulink model is developed to be more sensible when optimized with GSA, TLBO, and PSO algorithms, so that it is a little different from the Simulink model in [12]. Apparently, no study discusses the AGC performance subject to simultaneous small-step load perturbations at all. This investigation is an accurate comparison of the optimization of a three-unequal-area hydrothermal system using three novel evolutionary algorithms—GSA, TLBO, and PSO. Furthermore, it considers the effects of small-step load perturbation occurring in a single area as well as simultaneously in all the areas. All the case studies are considered with generation rate constraints (GRC) [12]. In light of this, the primary novelties of the present paper are as follows:

1. To simulate a three-unequal-area hydrothermal system which is more

sensible to the frequency and active power in all three areas.
2. To optimize the results of the simulation with three different practical heuristic algorithms (GSA, TLBO, PSO)
3. To compare the results obtained from the simulation with considering optimizing algorithms to the results obtained with the conventional integral controllers (without optimizing) [19].

Nomenclature

f nominal system frequency
i subscript referring to area (i = 1, 2, 3)
P_{ri} rated power of i^{th} area
ΔP_{tie} incremental change in tie-line power.
ΔP_{Di} incremental load change of i^{th} area.
ΔP_{gi} incremental generation change in i^{th} area.
Δf_i incremental change in frequency.
H_i inertia constant of i^{th} area
$D_i = \Delta P_{Di}/\Delta f_i$
T_{ij} synchronizing coefficient
R_i governor speed regulation parameter for i^{th} area
T_{ri} steam turbine reheat time constant for i^{th}area
T_{ti} steam turbine time constant for i^{th} area
T_{gi} speed governor time constant of i^{th} area
T_{pi} power system time constant of i^{th} area ($2H_i$/fD_i)
K_{pi} power system gain for i^{th} area ($1/D_i$)
K_{ri} steam turbine reheat coefficient for i^{th} area
ACE_i area control error of i^{th} area
B_i frequency bias for i^{th} area
K_D, K_p, K_i electric governor derivative, proportional, and integral gains respectively
T_w water starting time
$\beta_i = (D_i + 1/R_i)$ area frequency response characteristics for i^{th} area
$a_{ij} = -P_{ri}/P_{rj}$

2. Proposed method

The considered AGC system consists of three generating areas of equal size. Areas 1 and 2 are the reheat thermal systems and Area 3 is a hydro system. The characteristics of a hydro turbine differ from those of steam turbine in many aspects. The typical value of the permissible rate of generation for a hydro plant is especially support a large limitation between a typical value of GRC being 270% per minute for raising generation and 360% per minute for lowering generation [12]. Accordingly, Fig. 1 shows the AGC model of a three-area hydrothermal system developed for better simulation response in this research, as shown in Fig.6. The thermal plant has a single-stage reheat steam turbine and the hydro plant is equipped with an electric governor. A bias setting of $B_i = \beta_i$ is considered in both hydro and thermal areas [12, 19]. In this paper, the proposed AGC system [19] is optimized with three different algorithms for the first time. For all the simulations in this paper, MATLAB R2013b has been employed to carry out the dynamic responses when both frequency and tie-line power deviations are approximately 1% for the disturbance of step load in either area or simultaneously in all areas.

In order to optimize the simulation with three different evolutionary algorithms, it is first of all necessary to extend all the three algorithms. Subsequently, there is a brief definition of the mentioned algorithms, which is used in optimizing the AGC system in this paper.

A. Gravitational Search Algorithm (GSA)

The GSA could be considered as an isolated system of masses. It is like a small artificial world of masses that obey the Newtonian laws of gravitation and motion. More precisely, masses obey the following laws [20–21]:

Law of gravity: Each particle attracts every other particle and the gravitational force between two particles is directly proportional to the product of their masses and inversely proportional to the distance between them (R instead of R^2).

Law of motion: The current velocity of any mass is equal to the sum of the fraction of its previous velocity and the variation in the velocity. Variation in the velocity or acceleration of any mass is equal to the force acting on the system divided by mass of inertia.

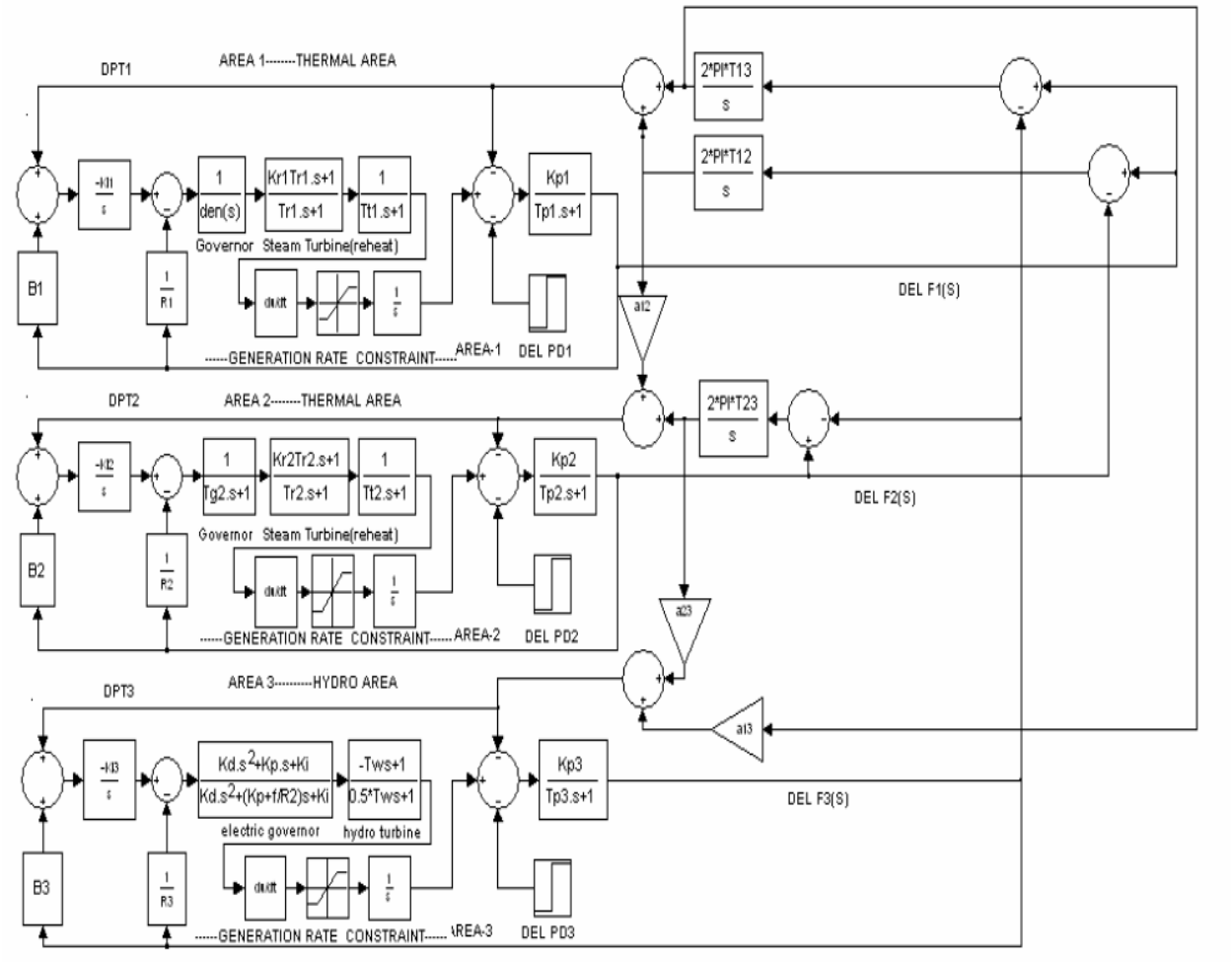

Fig. 1. Transfer function model of an interconnected three-area hydrothermal system [19]

Now, consider a system with N agents (masses). We define the position of the i^{th} agent by:

$$X_i = \left(x_i^1, \ldots, x_i^d, \ldots, x_i^n\right) \text{ for } i = 1,2,3,\ldots,N \quad (1)$$

where x_i^d presents the position of i^{th}agent in the d^{th} dimension.

At a specific time 't', the force acting on mass 'i' from mass 'j' is defined as follows:

$$F_{ij}^d(t) = G(t)\frac{M_{pi}(t) \times M_{aj}(t)}{R_{ij}(t) + \varepsilon}\left(x_j^d(t) - x_i^d(t)\right) \quad (2)$$

where M_{aj} is the active gravitational mass related to agent j, M_{pi} is the passive gravitational mass related to agent i, G(t) is gravitational constant at time t, ε is a small constant, and $R_{ij}(t)$ is the Euclidian distance between two agents i and j:

$$R_{ij}(t) = X_i(t).X_j(t)_2 \quad (3)$$

To give a stochastic characteristic to our algorithm, we suppose that the total force acting on agent i in a dimension d is a randomly weighted sum of d_{th} components of the forces exerted by other agents:

$$F_i^d(t) = \sum_{j=1, j\neq i}^{N} rand_j(t) F_{ij}^d(t) \quad (4.a)$$

$$F_i^d(t) = \sum_{j=k_{best}, j\neq i}^{N} rand_j(t) F_{ij}^d(t) \quad (4.b)$$

where randj is a random number in the interval [0, 1] and Kbest is the set of first K agents with the best fitness value and biggest mass. To improve the performance of GSA by controlling exploration and exploitation, only the Kbest agents will attract the others. Kbest is a function of time, with the initial value K0

at the beginning, and it decreases with time [22].

Hence, by the law of motion, the acceleration of the agent i at time t and in direction d^{th}, a_i^d(t), is given as follows:

$$a_i^d(t) = \frac{F_i^d(t)}{M_{ii}(t)} \tag{5}$$

where M_{ii} Inertial Mass of i^{th} agent.

Furthermore, the next velocity of an agent is considered as a fraction of its current velocity added to its acceleration. Therefore, its position and velocity can be calculated as follows:

$$V_i^d(t+1) = rand_i \times V_i^d(t) + a_i^d(t) \tag{6}$$

$$X_i^d(t+1) = X_i^d(t) + V_i^d(t+1) \tag{7}$$

The gravitational constant G is initialized at the beginning and will be reduced with time to control the search accuracy. In other words, G is a function of the initial value (G_0) and time (t):

$$G(t) = G(G_0, t) \tag{8}$$

Now the gravitational and inertial masses are updated by the following equations:

$$M_{ai} = M_{pi} = M_{ii} = M_i,\ i = 1,2,3,\ldots,N \tag{9}$$

$$m_i(t) = \frac{fit_i(t) - worst(t)}{best(t) - worst(t)} \tag{10}$$

$$M_i(t) = \frac{m_i(t)}{\sum_{j=1}^{N} m_j(t)} \tag{11}$$

where $fit_i(t)$ of the fitness value of the agent i at time t and worst(t) and best(t) are defined as follows (for a minimization problem):

$$best(t) = \min_{j \in \{1,2,\ldots,N\}} fit_j(t) \tag{12}$$

$$worst(t) = \max_{j \in \{1,2,\ldots,N\}} fit_j(t) \tag{13}$$

According to the mentioning formulation, the GSA flowchart is shown in Fig.2.

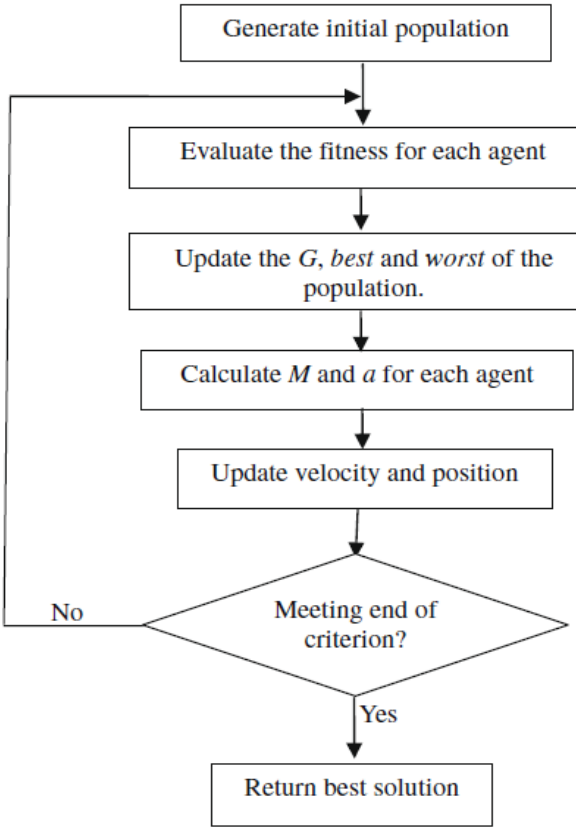

Fig. 2. Flowchart of GSA [20]

B. Teaching-Learning-Based Optimization (TLBO) algorithm

The TLBO algorithm [23, 24] was introduced by Rao et al. Since then, this algorithm has become a very popular and powerful optimization algorithm that is applied in many engineering fields. It is a nature-inspired algorithm that is based on the teacher-student interaction process in a class to generate a global solution. The working process of TLBO consists of two parts—the teacher phase and the learner phase.

In the teacher phase, students (learners) learn from teachers. In the learner phase, learners learn through interaction among themselves. The steps involved in the TLBO algorithm [23,24] are presented below.

i. Teacher phase

This phase of the algorithm simulates the learning of the students through a teacher. During this phase, the teacher conveys knowledge to the learners to improve the mean result of the class. Suppose there are 'm' subjects (i.e. design problems) offered to 'n' learners (i.e. population size k = 1, 2, 3, . . ., n). In the sequential teaching–learning process i, M_{ji} represents the mean results of the learners in a particular subject (j = 1, 2, . . ., m). Since the teacher is highly educated and experienced in that subject, the teacher is considered to be the best learner in the class. Let $X_{\text{total-kbest},i}$ be the result of the best learner considering all the subjects in the whole class; this is identified as the teacher of the class. The teacher will put in maximum effort to enhance the knowledge level of the entire class, but the knowledge gained by the learners will depend on the quality of teaching delivered by the teacher and quality of learners present in the class [25]. Considering this fact, the difference between the result of the teacher and mean result of the learners in each subject is expressed as [26]:

$$Difference\_mean_{jki} = r_i \left(X_{jkbesti} - T_F M_{ji} \right) \tag{14}$$

where X_{jkbesti} is the result of the best learner (i.e. the teacher) in the subject j, T_F is the teaching factor that decides the value of mean to be changed, and r_i is the random number in the range [0, 1]. T_F is not a parameter in this TLBO algorithm; its value can be either 1 or 2. The value of T_F is randomly decided as follows:

$$T_F = round\left(1 + rand\left(0,1\right)\right) \tag{15}$$

Based on this, the existing solution is updated according to the following equation:

$$X_{new,jki} = X_{old,jki} + Difference\_mean_{jki} \tag{16}$$

where $X_{old,jki}$ is the result of the learners in the class considering all the subjects and $X_{new,jki}$ is the updated value of $X_{old,jki}$. This is accepted if it gives a better value.

All the accepted function values at the end of the teacher phase are stored and are used as the input for the learner phase.

ii. Learner phase

Learners increase their knowledge through two different means— through input from the teacher or through interaction among themselves. A learner interacts randomly with other learners by means of group discussions, presentations, formal communications, etc. A learner learns something new if the other learner has more knowledge than him or her. Learner modification is expressed as follows: Two different learners, P and Q, are randomly selected such that $X_{new-total-Pj} \neq X_{new-total-Qj}$.

where $X_{new-total-Pj}$ and $X_{new-total-Qj}$ are the updated values of $X_{old-total-Pj}$ and $X_{old-total-Qj}$ respectively at the end of teacher phase.

$$\text{If } X_{new-total-Pj} < X_{new-total-Qj}$$
$$X'_{new-jpi} = X_{new-jpi} + r_i \left(X_{new-jQi} - X_{new-jPi} \right) \tag{17}$$

$$\text{If } X_{new-total-Pj} > X_{new-total-Qj}$$
$$X'_{new-jpi} = X_{new-jpi} + r_i \left(X_{new-jPi} - X_{new-jQi} \right) \tag{18}$$

$X'_{new-jpi}$ is accepted if it gives a better function value. The entire TLBO flowchart is shows in Fig.3.

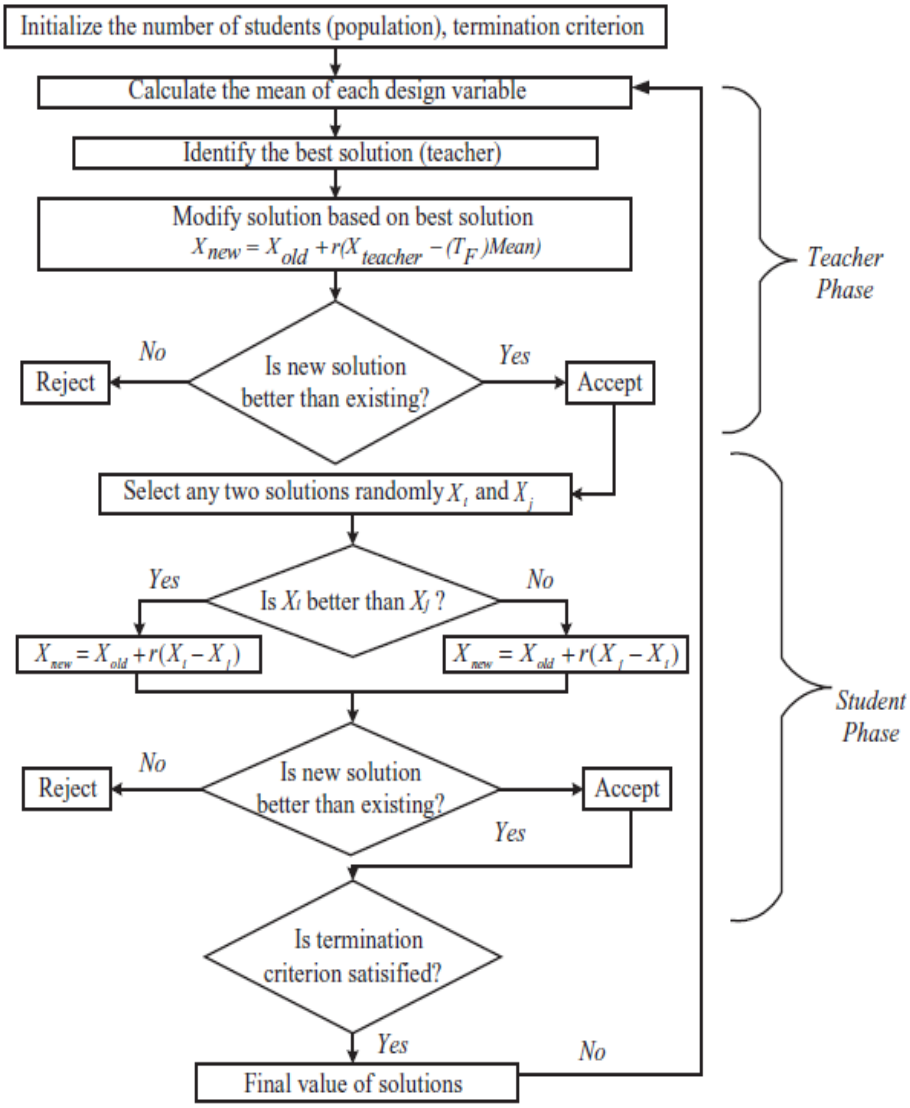

Fig.3. Flowchart of TLBO [3]

C. Particle Swarm Optimization (PSO) Algorithm

PSO—a population-based optimization algorithm—was first introduced by Kennedy and Eberhart in 1995 [27]. It can find high-quality solutions within shorter calculation time and with more stable convergence characteristics than other stochastic methods such as genetic algorithm, which involves a huge number of massive calculations as well as programming heavy codes to optimize an AGC problem.

PSO uses particles that represent potential solutions of the problem. Each particle flies in the search space at a certain velocity, which can be adjusted in light of preceding flight experiences. The projected position of the ith particle of the swarm x_i, and the velocity of this particle v_i at $(t + 1)$th iteration are defined and updated as the following two equations:

$$v_i^{t+1} = v_i^t + c_1 r_1 \left(p_i^t - x_i^t\right) + c_2 r_2 \left(g_i^t - x_i^t\right) \qquad (19)$$

$$x_i^{t+1} = x_i^t + v_i^{t+1} \qquad (20)$$

where i = 1,…, n and n is the size of the swarm, c_1 and c_2 are positive constants, r_1 and r_2 are random numbers that are uniformly distributed in [0, 1], t determines the iteration number, p_i represents the best previous position (the position giving the best fitness value) of the ith particle, and g represents the best particle among all the particles in the swarm. At the end of the iterations, the best

position of the swarm will be the solution to the problem. It cannot always be possible to get an optimum result of the problem, but the obtained solution will be an optimal one [28]. The PSO flowchart is shown in Fig.4.

3. Case study simulation

Generally, in a multi-area system, load perturbation can occur anywhere either in one area or in a few areas or in all areas concurrently. The literature survey shows that researchers have considered a typical value of 1% step load perturbation in an area to optimize the gain for the conventional integral controller in the AGC model. Hence, it is important for this study to investigate whether the optimum gain obtained with step load perturbation in an area could be acceptable for step load perturbation when this disturbance simultaneously occurs in all the areas. For this reason, the desire values for optimizing the three-area hydrothermal AGC are listed in Appendix A.

Additionally, the AGC system, which is improved in comparison to the model shown in Fig.1, is shown below (Fig.5). This model consists of three ACE parts that show the error inputs to the controllers.

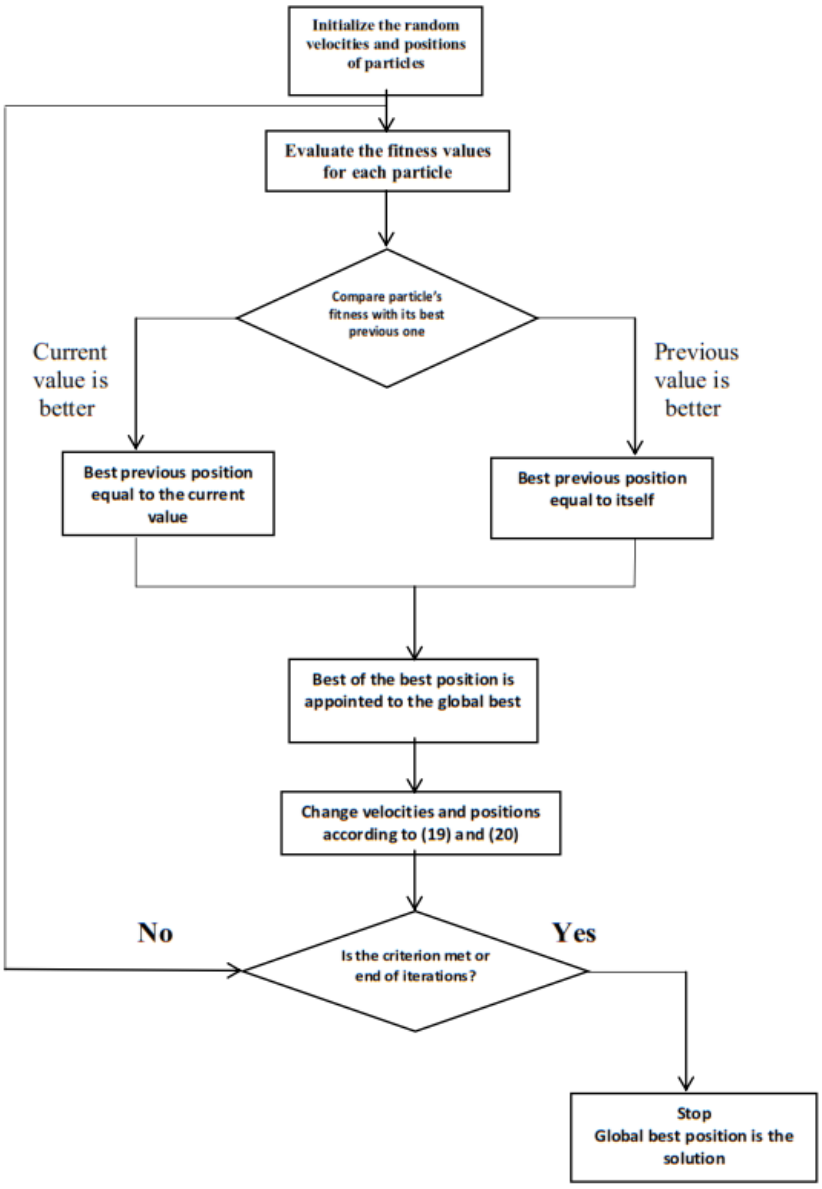

Fig. 4. The flowchart of the standard PSO algorithm [28].

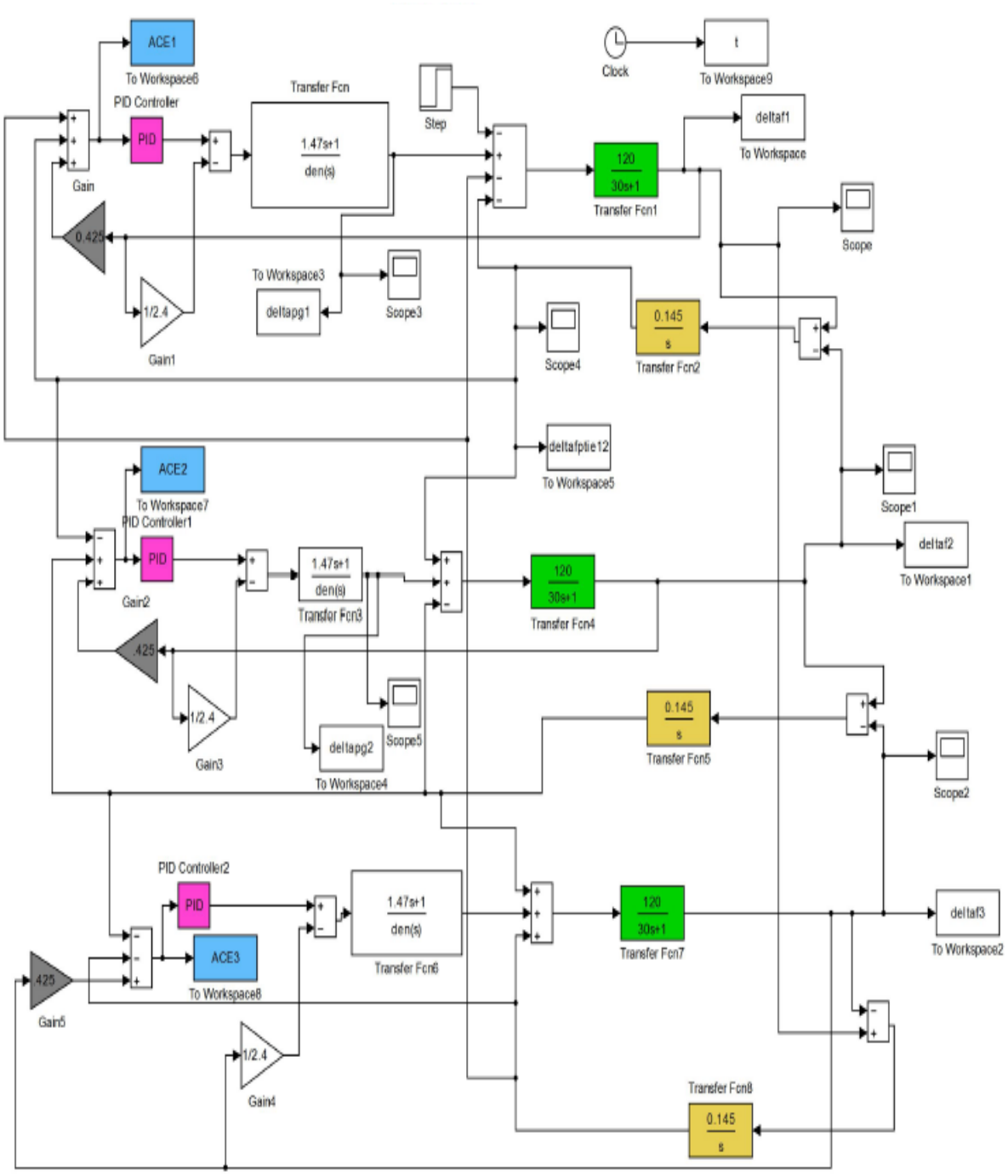

Fig.5. The novel improved transfer function model of an interconnected three-area hydrothermal system used in simulation.

In this paper, simulations were conducted on an Intel Core i-7 CPU of 2.2 GHz, 16 GB, 64-bit processor computer in the MATLAB 8.1.0.604 (R2013a) environment. First, a brief review is given of the simulation results of AGC with conventional integrals controllers [19], which are obtained from simulation model shown in Fig.5.

In this section, the simulation results applying optimization algorithms TLBO, GSA, and PSO are depicted in Figs. 10–13.

Table 1 shows some comparisons depicted in the above figures.

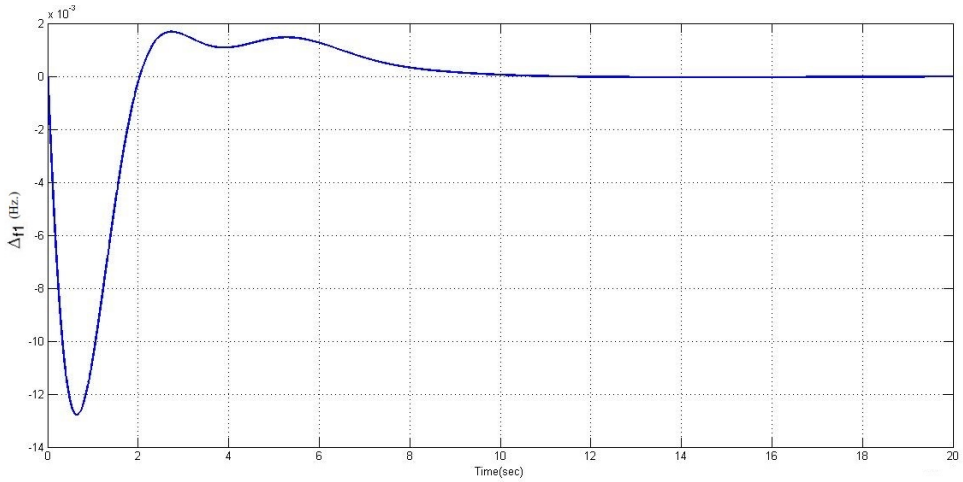

Fig. 6. The frequency deviation in Area 1 with conventional integrals (without optimizing)

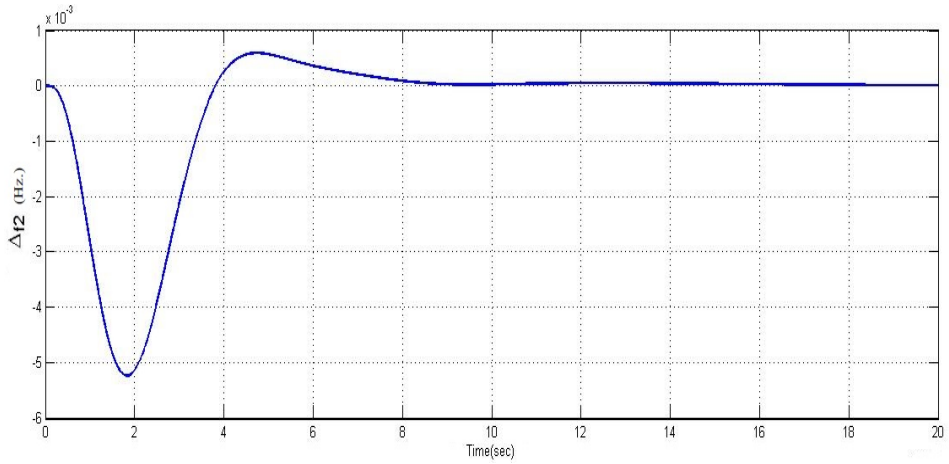

Fig. 7. The frequency deviation in Area 2 with conventional integrals (without optimizing)

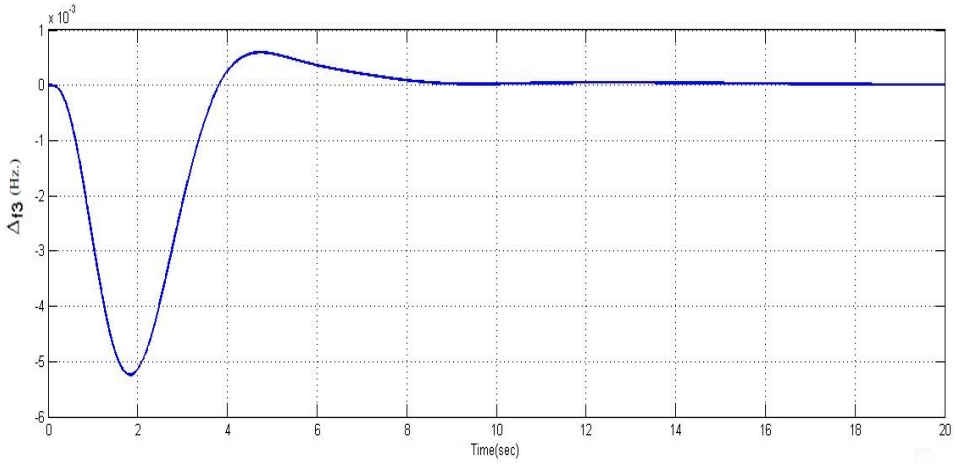

Fig. 8. The frequency deviation in Area 3 with conventional integrals (without optimizing)

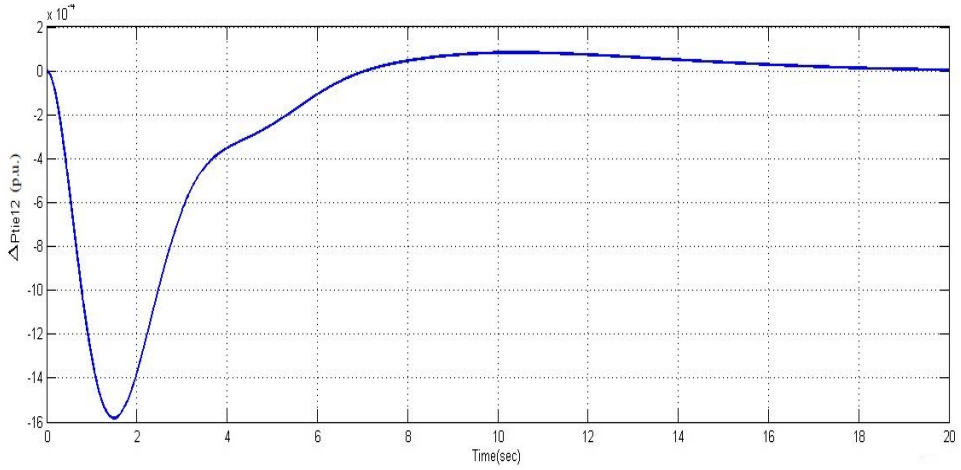

Fig. 9. The tie-line power deviation between Areas 1 and 2 with conventional integrals (without optimizing)

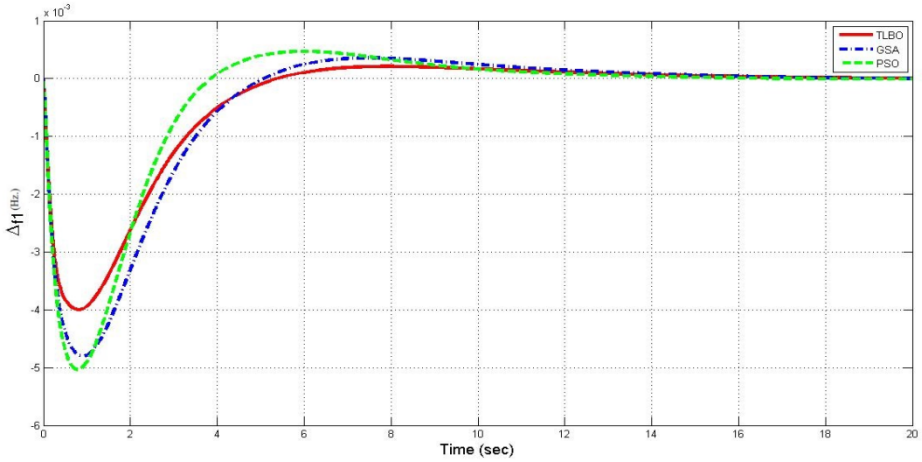

Fig. 10. Comparison of the frequency deviation in Area 1 under optimization by means of TLBO, GSA, and PSO algorithms

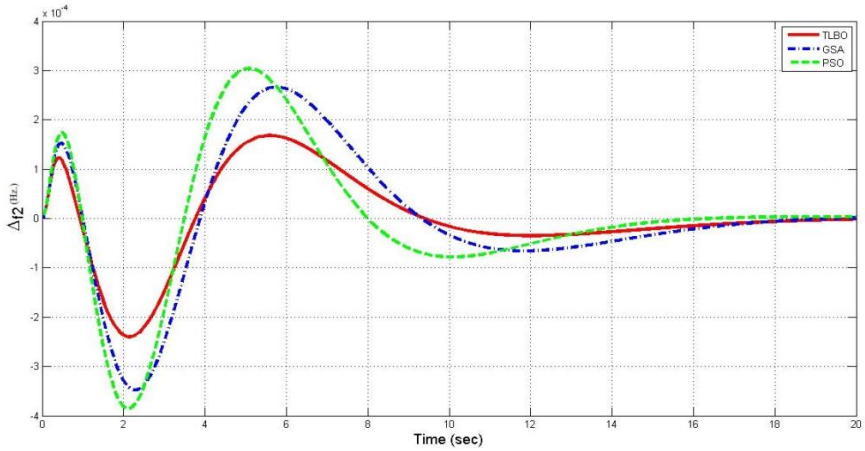

Fig. 11. Comparison of the frequency deviation in Area 2 under optimization by means of TLBO, GSA, and PSO algorithms

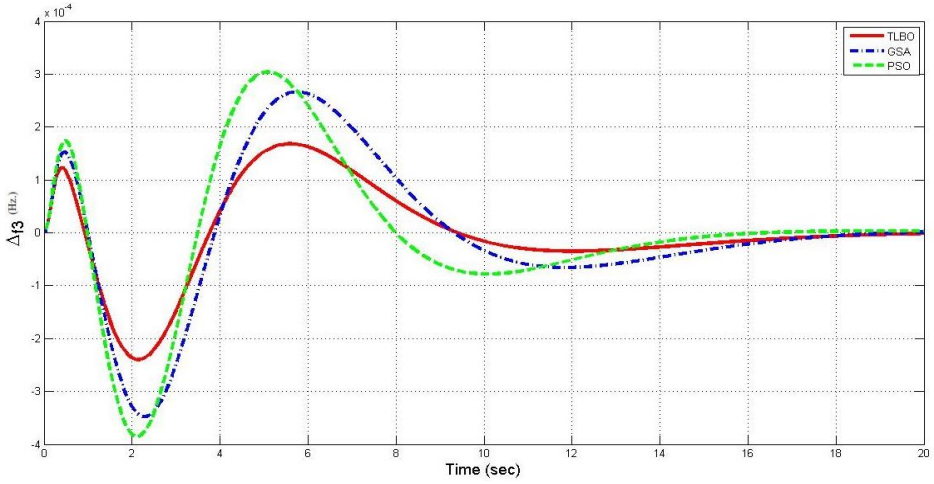

Fig. 12. Comparison of the frequency deviation in Area 3 under optimization by means of TLBO, GSA, and PSO algorithms

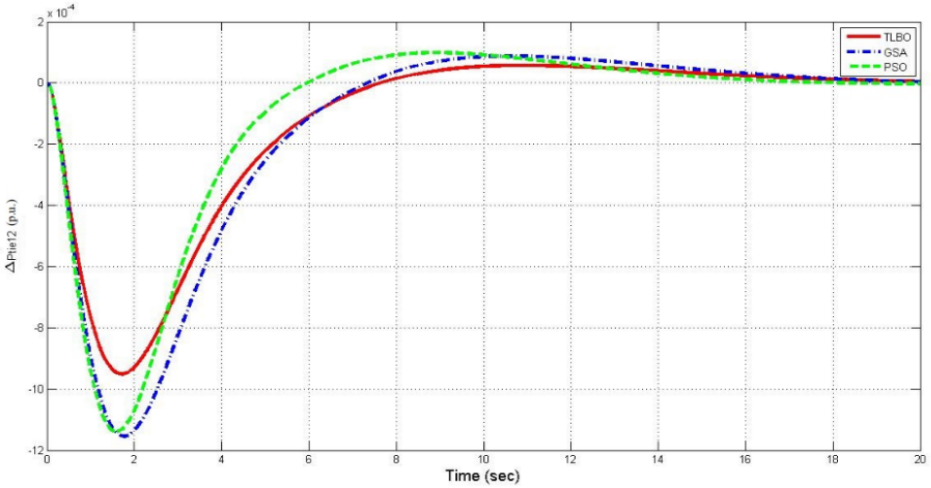

Fig. 13. Comparison of the tie-line power deviation between Areas 1 and 2 under optimization, by means of TLBO, GSA and PSO algorithms

Table 1. Comparison of the numerical results obtained both without optimizing and optimizing with TLBO, GSA, and PSO algorithms

Frequency Deviation (Hz)		**without optimization**	**TLBO**	**GSA**	**PSO**
Δf_1	Min	- 0.01279	- 0.003999	- 0.004805	- 0.005034
	Max	0.00168	0.0002095	0.0003571	0.0004707
Δf_2	Min	- 0.005243	- 0.0002399	- 0.0003477	- 0.0003855
	Max	0.0005931	0.0001681	0.0002661	0.0003038
Δf_3	Min	- 0.005243	- 0.0002399	- 0.0003477	- 0.0003855
	Max	0.0005931	0.0001681	0.0002661	0.0003038
Active Power Deviation		without optimization	TLBO	GSA	PSO
ΔP_{tie12}	Min	- 0.001583	- 0.0009511	- 0.001155	- 0.00114
	Max	8.284e-05	5.713e-05	8.792e-05	9.891e-05

It should be mentioned that in all three areas, the amount of step load perturbation is considered to be equal to 1%. Accordingly, as shown in Fig.10, the frequency deviation values in Area 1 (Δf_1) under optimization applying TLBO, GSA, and PSO algorithms are

0.0042085, 0.0051621, and 0.0055047 (Hz) respectively. A similar pattern can be seen in the other simulation curves. To explain more, in Area 2, the alteration of frequency (Δf_2)), under TLBO, GSA and PSO algorithms is 0.000408, 0.0006138 and 0.0006893 (Hz), respectively. In comparison with previous curves (Δf_2)), as can be seen in Figs. 11 and 12, the frequency deviation in Area 3 (Δf_3)) is approximately similar to that shown in Fig. 11. As shown in Fig.13, the tie-line power deviation values between Areas 1 and 2 (ΔP_{tie12}) under optimization by means of employed algorithms including TLBO, GSA, and PSO are equal to 0.00100823, 0.00124292, and 0.00123891 (p.u.), respectively.

Also, the frequency deviation and tie-line power deviation are noticeably much higher compared to the optimization results. According to Figures 6–9; the frequency deviation values in Area 1 (Δf_1)), Area 2 (Δf_2)), and Area 3 (Δf_3)) and the deviation values of tie-line power between Area 1&2 (ΔP_{tie12}) are 0.01447, 0.0058361, 0.0058361 Hz, and 0.00166584 (p.u.) respectively. Hence, comparison between the obtained results makes it obvious that the TLBO is the best optimizing algorithm among the presented evolutionary algorithms. This is mainly due to its better behavior in terms of frequency deviation in all three areas as well as the tie-power deviation between Areas 1&2.

On the other hand, the peak points of the simulated curves are significantly crucial for investigating the power and frequency stability. To determine these points, first, one should refer to Figs. 6–9. The maximum value of the frequency deviation in Area 1 (Δf_1)) is 0.00168 (Hz). Similarly, the deviation values of frequency in Area 2 (Δf_2)) & 3(Δf_3)), apart from the deviation of the tie-line power between Areas 1 and 2 (ΔP_{tie12}), reach their highest points at 0.0005931, 0.0005931 (Hz), and 8.284e-05 (p.u.). These peak points are optimized with TLBO, GSA, and PSO algorithms as shown in Figs. 10–13. According to the figures, under optimization by applying TLBO algorithm, the values of (Δf_1)), (Δf_2)), (Δf_3)), and (ΔP_{tie12}) have the peak of 0.0002095, 0.0001681, and 0.0001681 (Hz), and 5.713e-05 (p.u.). Moreover, when the AGC system is optimized using GSA algorithm, these parameters are 0.0003571, 0.0002661, 0.0002661 (Hz), and 8.792e-05 (p.u.) respectively. In the same way, while employing the PSO algorithm to optimize the AGC system, the mentioned characters hit a peak of 0.0004707, 0.0003038, 0.0003038 (Hz), and 9.891e-05 (p.u.) respectively. It is evident that the TLBO algorithm has the lowest peak point in all four simulated parameters, which results in best stability while using this AGC system.

Another important factor is the settling time. Therefore, it is necessary to determine a reference time to measure the deviation of frequency and tie-line power from zero point. In this paper, the reference time is set to 10 seconds. In contrast to the zero point at the defined criterion for time (10s), at first, the deviation values of frequency in Area 1(Δf_1)) for the simulations obtained using TLBO, GSA, and PSO algorithms are 0.0001673, 0.0002446, and 0.0001633 (Hz). This parameter, without considering evolutionary algorithms, is 5.505e-05 (Hz). This trend could be similarly employed to extend the frequency deviation in Area 2 (Δf_2)) & 3 (Δf_3)) and the tie-line power deviation between Areas 1 and 2 (ΔP_{tie12}). The frequency deviation values in Area 2 (Δf_2)) from zero point at the 10th second, under optimization with TLBO, GSA, and PSO algorithms are −1.625e-05, −3.372e-05, and −7.803e-05 (Hz); additionally, the value of this parameter is 2.442e-05 (Hz) without optimizing methods. These values are almost acceptable for frequency deviation in Area 3. At last, the tie-line power deviation between Areas 1 and 2 is analyzed. According to Figs. 9 and 13, this parameter's values, when applying TLBO, GSA and PSO algorithms, are 5.423e-05, 8.593e-05, and 9.179e-05 (p.u.) respectively. In addition, the value is 8.199e-05 (p.u) without any optimization. Finally, it could be concluded that by employing the TLBO algorithm, the deviation of frequency and tie-line power between Areas 1 and 2 from zero point will be lower at the 10th second in comparison to GSA and PSO algorithms.

4. Result and discussion

In this paper, the AGC system of a hydrothermal system based on modelling the appropriate generation rate constraints is presented. For this purpose, the integral controllers and electric governor parameters are optimized using ISE criterion. Also, some evolutionary algorithms such as TLBO, PSO, and GSA are applied for optimizing the AGC

performance. Analysis of the obtained data confirms that applying evolutionary algorithms to this problem leads to better performances in general. Furthermore, the detailed analysis shows the ability of TLBO algorithm in finding the better solution compared to other algorithms.

References

[1] Elgerd O.I., Electric Energy Systems Theory– An Introduction, Second Edition, Tata McGraw Hill, New Delhi (2000).

[2] Kundur P., Power System Stability and Control, Eighth Reprint, Tata McGraw Hill, New Delhi (2009).

[3] Sahu R. K., Gorripotu T. S., Panda S., Automatic Generation Control of Multi-Area Power Systems with Diverse Energy Sources Using Teaching Learning Based Optimization Algorithm, Engineering Science and Technology, an International Journal (2016) 19(1):113-134.

[4] Parmar K. S., Majhi S., Kothari D. P., Load Frequency Control of a Realistic Power System with Multi-Source Power Generation, International Journal of Electrical Power & Energy Systems (2012) 42(1):426-433.

[5] Bhatt P., Ghoshal S. P., Roy R., Load Frequency Stabilization by Coordinated Control of Thyristor Controlled Phase Shifters and Superconducting Magnetic Energy Storage for Three Types of Interconnected Two-Area Power Systems, International Journal of Electrical Power & Energy Systems(2010) 32(10): 1111-1124.

[6] Rout U. K., Sahu R. K., Panda S. Design and Analysis of Differential Evolution Algorithm Based Automatic Generation Control for Interconnected Power System, Ain Shams Engineering Journal (2013) 4(3):409-421.

[7] Panda S., Yegireddy N. K. Automatic Generation Control of Multi-Area Power System Using Multi-Objective Non-Dominated Sorting Genetic Algorithm-II, International Journal of Electrical Power & Energy Systems (2013) 53:54-63.

[8] Saikia L. C., Nanda J., Mishra S., Performance Comparison of Several Classical Controllers in AGC for Multi-Area Interconnected Thermal System, International Journal of Electrical Power & Energy Systems (2011) 33(3): 394-401.

[9] Taher S. A., Fini M. H., Aliabadi S. F. Fractional Order PID Controller Design for LFC in Electric Power Systems Using Imperialist Competitive Algorithm, Ain Shams Engineering Journal (2014) 5(1): 121-135.

[10] Debbarma S., Saikia L. C., Sinha N. Robust Two-Degree-of-Freedom Controller for Automatic Generation Control of Multi-Area System, International Journal of Electrical Power & Energy Systems (2014) 63: 878-886.

[11] Daneshfar F., Bevrani H. Multi Objective Design of Load Frequency Control Using Genetic Algorithms, International Journal of Electrical Power & Energy Systems (2012) 42(1):257-263.

[12] Khuntia S. R., Panda S., Simulation Study for Automatic Generation Control of a Multi-Area Power System by ANFIS Approach, Applied soft computing (2012) 12(1):333-341.

[13] Bhatt P., Roy R., GhoshalS. P., GA/Particle Swarm Intelligence Based Optimization of Two Specific Varieties of Controller Devices Applied to Two-Area Multi-Units Automatic Generation Control, International Journal of Electrical Power & Energy Systems (2010) 32(4):299-310.

[14] Bhatt P., Roy R., Ghoshal S. P., Optimized Multi Area AGC Simulation in Restructured Power Systems, International Journal of Electrical Power & Energy Systems (2010) 32(4): 311-322.

[15] Kumar L. S., Kumar G. N., Madichetty S., Pattern Search Algorithm Based Automatic Online Parameter Estimation for AGC with Effects of Wind Power, International Journal of Electrical Power & Energy Systems (2017) 84:135-142.

[16] Guha D., Roy P. K., Banerjee, S., Study of Differential Search Algorithm Based Automatic Generation Control of an Interconnected Thermal-Thermal System with Governor Dead-Band, Applied Soft Computing (2017) 52:160-175.

[17] Hota P. K., Mohanty B., Automatic Generation Control of Multi Source Power Generation under Deregulated Environment, International Journal of Electrical Power & Energy Systems(2016) 75:205-214.

[18] Jagatheesan K., Anand B., Samanta S., Dey N., Ashour A. S., Balas V. E. Design of a Proportional-Integral-Derivative Controller for an Automatic Generation Control of Multi-Area Power Thermal Systems Using Firefly Algorithm, IEEE/CAA Journal of Automatica Sinica(2017).

[19] Nanda J., Parida M., Kalam A., Automatic Generation Control of a Multi-Area Power System with Conventional Integral Controllers (2006).

[20] Rashedi E., Nezamabadi-Pour H., Saryazdi S., GSA: A Gravitational Search Algorithm, Information Sciences (2009) 179(13): 2232-2248.

[21] Elsisi M., Soliman M., Aboelela M. A. S., Mansour W., GSA-Based Design of Dual Proportional Integral Load Frequency Controllers for Nonlinear Hydrothermal Power System. World Academy of Science, Engineering and Technology, International Journal of Electrical, Computer, Energetic,

Electronic and Communication Engineering (2015) 9(8):928-934.
[22] Sharma D., Kumar M., SinghA. K., Improved PI using GSA Algorithm for LFC of Two Area Thermal Power System (2017).
[23] Rao R. V., Savsani V. J., Vakharia D. P. Teaching–Learning-Based Optimization: An Optimization Method for Continuous Non-Linear Large Scale Problems, Information Sciences (2012) 183(1):1-15.
[24] Rao R. V., Savsani V. J., Vakharia D. P. Teaching–Learning-Based Optimization: A Novel Method for Constrained Mechanical Design Optimization Problems, Computer-Aided Design (2011) 43(3):303-315.
[25] Mohanty B., TLBO Optimized Sliding Mode Controller for Multi-Area Multi-Source Nonlinear Interconnected AGC System, International Journal of Electrical Power & Energy Systems(2015)73:872-881.
[26] Roy P. K., Teaching Learning Based Optimization for Short-Term Hydrothermal Scheduling Problem Considering Valve Point Effect and Prohibited Discharge Constraint, International Journal of Electrical Power & Energy Systems (2013) 53:10-19.
[27] Kennedy R. J., Eberhart, Particle Swarm Optimization, In Proceedings of IEEE International Conference on Neural Networks IV (1995) 1000.
[28] Gozde H., TaplamaciogluM. C. Automatic Generation Control Application with Craziness Based Particle Swarm Optimization in a Thermal Power System, International Journal of Electrical Power & Energy Systems(2011) 33(1):8-16.

Appendix A

Nominal parameter of the unequal three-area hydrothermal system [12,19]:
$P_{r1}=P_{r2}=P_{r3}=2000$ MW;
$H_1=H_2=H_3=5$ Seconds
$D_1=D_2=D_3=8.33*10^{-3}$ P.U.MW/Hz;
$K_{r1}=K_{r2}=0.5$
$R_1=R_2=R_{3=}2.4$ Hz/P.U.MW;
$T_{r1}=T_{r2}=10$ Seconds
$K_{p1}=K_{p2}=K_{p3}=120$Hz/P.U.MW;
$T_{p1}=T_{p2}=T_{P3}=20$ Seconds
$T_{12}=T_{13}=T_{23}=0.086$p.u.MW/Radian;
F=60 Hz; $P_{tie,\ Max}=200$ MW;
Tw=1 sec.; $a_{12}=a_{13}=a_{23}=-1$;
$T_{g1}=T_{g2}=0.08$ Seconds;
$T_{t1}=T_{t2}=0.3$ Second;
Initial loading: $P_{D1}^{0}=P_{D2}^{0}=P_{D3}^{0}=1000$ MW
$K_{I1}=0.111$, $K_{I2}=0.111$, $K_{I3}=0.027$ for simultaneous step load perturbation
$K_{I1}=0.155$, $K_{I2}=0.155$, $K_{I3}=0.049$ for step load perturbation occurring in an area